

Evaluating H₂ Infiltration via Drone-Based Thermal Imaging

Luca Imponenti¹[\[https://orcid.org/0000-0003-1628-5779\]](https://orcid.org/0000-0003-1628-5779), Keith Boyle¹[\[https://orcid.org/0000-0002-6436-0684\]](https://orcid.org/0000-0002-6436-0684), Ryan Shinger¹, Tim Wendelin¹ and Hank Price¹[\[https://orcid.org/0000-0002-6704-9197\]](https://orcid.org/0000-0002-6704-9197)

¹ Solar Dynamics LLC

Abstract. This work discusses the analysis of thermal survey data from operating parabolic trough plants. A thermal survey consists of IR images of individual HCEs in a parabolic trough collector, these images are the basis of a non-intrusive methodology for evaluating the heat losses. The HCE performance is affected by issues such as H₂ infiltration and lost vacuum, which are difficult to identify visually but significantly increase the heat losses. In this work the glass temperatures from survey data are compared to predictions from a reduced order model of the HCE with good agreement. The model is then used for parametric studies looking at the variation of important ambient conditions, glass envelope conditions, and optical properties. Results indicate the model is a useful and computationally efficient tool to determine the status of a given HCE; however, it can be difficult to distinguish between lost vacuum (from outside air infiltration), and certain levels of H₂ infiltration (from decomposition of the HTF). The main methodology for identifying H₂ infiltration in these cases involves thermal surveying at different times of the day, taking advantage of the temperature dependence of the getter capacity.

Keywords: Parabolic Trough, Receiver, Heat Collection Element (HCE), Hydrogen

1. Introduction

The major issue affecting the performance of operating parabolic trough plants is hydrogen (H₂) infiltration of the receiver tube, according to the Concentrating Solar Power Best Practices Study [1]. Infrared (IR) cameras are useful tools to assess the extent of this issue at operating plants. Thermal images of the receiver glass envelope from these cameras are a non-intrusive measurement of thermal energy in a portion of the infrared spectrum, that can be analyzed to evaluate the performance and status of receiver tubes, also known as Heat Collector Elements (HCEs). Combining an IR camera with Unmanned Aerial Vehicles (UAVs or drones) allows large solar fields to be covered in a fraction of the time compared to ground-based surveying [2]. This work explores the different factors affecting HCE performance and the challenges associated with accurate identification of issues via UAV data collection.

The glass envelope temperature is an indicator of the thermal losses from the HCE. Although the actual losses depend on operating and ambient conditions, for a given set of conditions, a higher glass temperature indicates higher losses. Several factors can increase thermal losses of an HCE installed in the solar field, including:

- H₂ infiltration into vacuum space from heat transfer fluid (HTF) degradation.
- Broken glass envelope leaving an exposed absorber tube.
- Outside air infiltration due to lost vacuum.
- Degradation of absorber tube coating.

- Degradation of getter material generating 'dust' within the glass envelope.

Of these, H₂ infiltration and loss of vacuum are challenging to identify with the naked eye; however, the thermal losses in both cases are higher than normal and can be captured by an IR camera. While loss of vacuum can be considered a component failure, H₂ infiltration is a known issue that arises due to the decomposition of the oil based HTF [1, 3]. To alleviate this issue getters are installed in the vacuum space of the HCE to absorb H₂ up to a certain partial pressure, P_{H_2} . Eventually the getter capacity, which is a function of temperature, is reached and H₂ can be found in the vacuum space. Hotter HCEs tend to saturate faster due to the higher permeation of H₂ through the absorber tube and the reduced getter capacity at higher temperature [3].

To accurately assess each case, it is helpful to understand how each issue impacts the temperature of the glass envelope. Previous modeling studies include a 1D analytical model commonly used for plant performance modeling [4], and more in-depth 3D CFD and FEA analysis to evaluate temperature gradients and stresses [5, 6]. Leveraging previous modeling efforts, the status of HCEs in the solar field may be determined through analysis of high-quality thermal images.

2. Data Collection

HCE temperatures are extracted from IR images by filtering an image down to a set of pixels that represent the HCE and calculating a single (summary) temperature value through a statistical analysis. Images are collected during plant operation when the HCEs are at operating temperature, providing more relevant data for evaluating performance. Calculating a single temperature for the HCE is often challenging due to the presence of real temperature gradients along the length and circumference of the HCE, as well as measurement anomalies due to glare/glint, dirty spots, or stray reflections, as shown in Figure 1. Previous ground-based surveys considered the maximum temperature of the HCE [2]; however, the images in this case are less consistent due to the collection method, and glare is less of an issue when imaging from the ground. The current methodology considers the maximum temperature along the circumference of the tube, and the median temperature along the length of the tube. By selecting the maximum temperature around the circumference, the effect of the cold mirror pixels near the edge of the HCE is minimized, whereas the median temperature is necessary along the length to avoid false hot spots attributed to glare and other anomalies.

The IR camera measures the thermal energy in the framed image, this signal is then analyzed to calculate the temperature of that image. The calculated temperature depends on several factors including: temperature of the target and surroundings, optical properties of the target, and atmospheric attenuation of the IR signal. The uncertainty of this calculation results in a temperature measurement accuracy around $\pm 3^\circ\text{C}$, assuming correct parameters are input, based on test images collected of a known temperature object. The IR images in Figure 1 demonstrate how incorrect properties can have a drastic effect, since the bellow shields have different optical properties than the glass envelope they look like the coldest object in the image. For consistency ideal IR images are framed with the camera looking into the aperture of the collector, as shown in Figure 1(a), and must be close enough to capture a sufficient number of pixels across the HCE diameter for a reliable temperature measurement. The required number of pixels will vary based on the camera optical properties and collector geometry, in this case approximately ten pixels. When looking directly into the aperture the measured glass temperature will be the top of the glass, i.e., the portion of the HCE opposite of the parabolic mirrors. In this work the bottom of the HCE refers to the portion of the HCE nearest the vertex of the parabola.

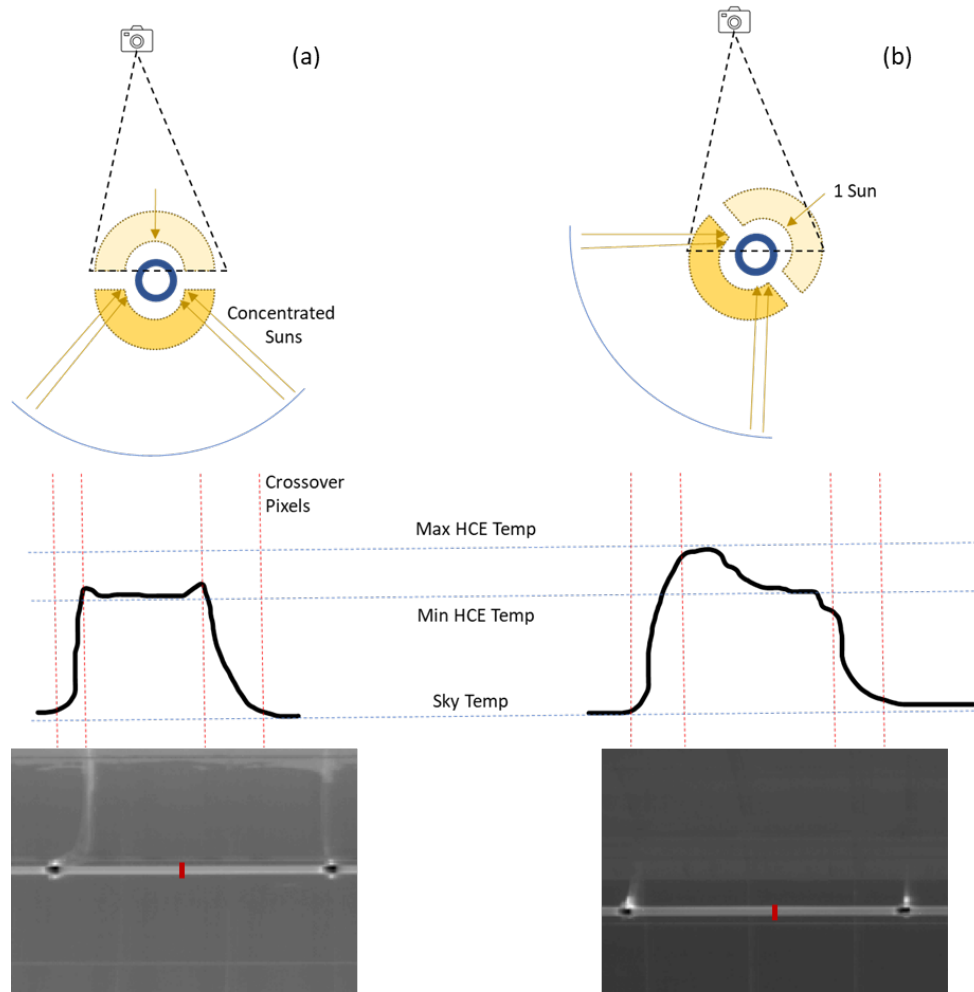


Figure 1. Example of IR images of HCEs taken with a drone at different angles, and representative temperature profiles.

3. HCE Modelling

To best interpret results from a thermal survey of the solar field, it is useful to model and understand the heat losses. Due to the sheer number of HCEs in a typical commercial solar field it is not feasible to use CFD modelling to evaluate each case. A 1D analytical model from NREL is ideal for this type of data analysis [4]. The 1D formulation has been proven accurate for predicting the total heat losses from the receiver [7]; however, the model cannot resolve the circumferential temperature gradient around the receiver. There is effectively a large difference in the solar heat input between the top and bottom of the receiver. For the purposes of this analysis the solar heat input which provided the best agreement with selected thermal survey data was used; this selection is discussed in the next section. Another limitation of the model involves the correlation for molecular heat transfer within the glass envelope: in this model the thermal accommodation coefficients are assumed to be 1, resulting in the maximum energy exchange between the gas molecule and the surface [8].

In addition to these model limitations, environmental conditions and optical properties are the most sensitive parameters affecting the modelled glass temperature. The optical properties of the HCE are usually well known within some variability of the manufacturing process; however, soiling of the glass envelope and degradation of the selective coating can change the effective optical properties. Environmental conditions such as localized wind speed and the sky temperature can also be challenging to quantify. An average wind speed is usually available from the plant data, but localized gusts impact the instantaneous temper-

ature reading through the IR camera. The effective sky temperature is also a parameter that can be calculated based on weather data and solar position [9], but cloud cover and other obstructions result in a more localized value. All these factors introduce uncertainty in the analysis that must be considered when evaluating the HCE performance.

4. Results & Discussion

4.1 Thermal Survey Data

The modelled glass temperature is compared to measured values from a large sample of survey data in Figure 2; all the data points plotted are for 'healthy' HCEs with no known defects or maintenance issues. Using the average solar heat input of 5250 W/m and a collector efficiency of 0.8 results in a mean error of 1.4°C with a standard deviation of 2.9°C, considering over 20000 sample points. Although the maximum error is 19.5°C, the mean value and standard deviation are within the expected accuracy of the IR-based temperature measurement. The outliers and some level of variance in the data is expected due to uncertainty in operational and ambient conditions as previously discussed. The 1D model shows good agreement with the data at lower values of ΔT , which generally corresponds to lower heat loss conditions; however, as the heat losses increase the mean error also increases from 0.7°C for $\Delta T < 20^\circ\text{C}$ to 4.7°C for $\Delta T \geq 20^\circ\text{C}$. The increased error under higher heat loss conditions is attributed to the 1D model formulation and associated simplifications in the natural convection heat transfer between the outer receiver wall and inner glass surface. Despite this increase a mean error around 5°C is of similar magnitude to the temperature measurement uncertainty and considered acceptable for diagnosis of the surveyed HCEs; however, the accuracy of the model under high heat loss conditions will need to be evaluated more thoroughly to improve the confidence of predictions in this regime.

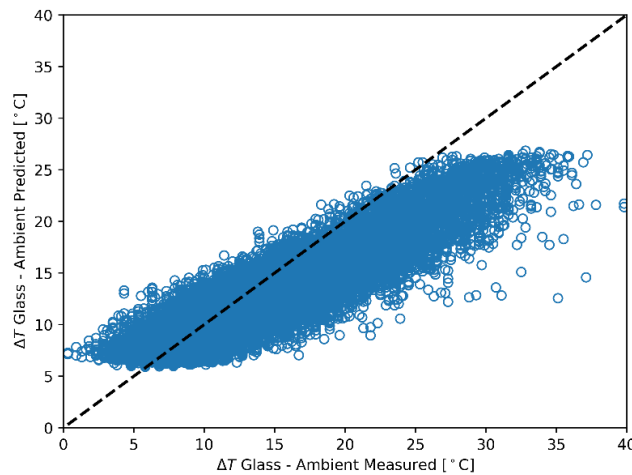


Figure 2. Sample survey data compared to Forristall model results.

In cases like Figure 1(b) a temperature gradient on the order of 15°C has been observed across the visible circumference of the HCE. Based on the data in Table 1 and Figure 2, a change in temperature of 15°C is significant for evaluating the HCE performance. Thus, it is important to consider high quality images with correct framing for a high-fidelity analysis. High quality sample thermal survey data is presented in Table 1. The glass temperature is the measured value calculated from the thermal images, while the HTF and weather data is provided by the surveyed plant and the sky temperature is calculated from these parameters. The cases selected are different HCEs with varying levels of thermal losses located in different positions of the loop for analysis. The recorded ambient conditions are similar for all the selected cases, despite this there is a large spread in the measured temperature data. Due

to the multimode heat transfer occurring in the HCE, the model helps understand heat loss trends and interpret the thermal survey results. Model results are compared to the cases from Table 1 in the following sections.

Table 1. Representative thermal survey data: glass temperature determined from analysis of IR images, HTF and weather data provided by plant.

Case	Glass T [°C]	HTF T [°C]	Ambient T [°C]	Sky T [°C]	Wind Speed [m/s]
1	39	300.1	36.2	18.7	2.2
2	57	300.8	35.9	18.5	2.2
3	77	299.8	34.9	17.7	3.9
4	47	379.2	35.7	18.9	3.8
5	67	382	32.5	15.4	2.2
6	93	378.6	33	15.8	3

4.2 Glass Envelope Conditions

The 1D model [4] is used to evaluate the HCE heat losses under different glass envelope conditions relevant for the thermal survey cases in Table 1. In Figure 3 model results are plotted comparing the top of glass temperature for different envelope pressures, P_{vac} , of hydrogen and air at different HTF temperatures; the conditions selected for each plot are the average values of the survey cases included with the dotted lines. Similar trends can be observed as the annular space in the glass envelope is pressurized, although the losses are significantly higher with H₂. Initially as P_{vac} increases the heat losses also increase due to free molecular heat transfer, this mode of heat transfer reaches a limit around 0.01 bar for hydrogen compared to 0.001 bar for air. The thermal properties of H₂ increase the glass temperature significantly more than air in this regime. As P_{vac} approaches ambient, natural convection takes over as the dominant mode of heat transfer. This transition occurs around 0.1 bar for air and close to ambient pressure for hydrogen. A previous study modeling the H₂ build-up in a parabolic trough plant considers the HCE in need of replacement when the H₂ pressure in the annulus reaches 0.01 bar [3]; referencing Figure 3, at this pressure the heat losses due to free molecular heat transfer reach their peak.

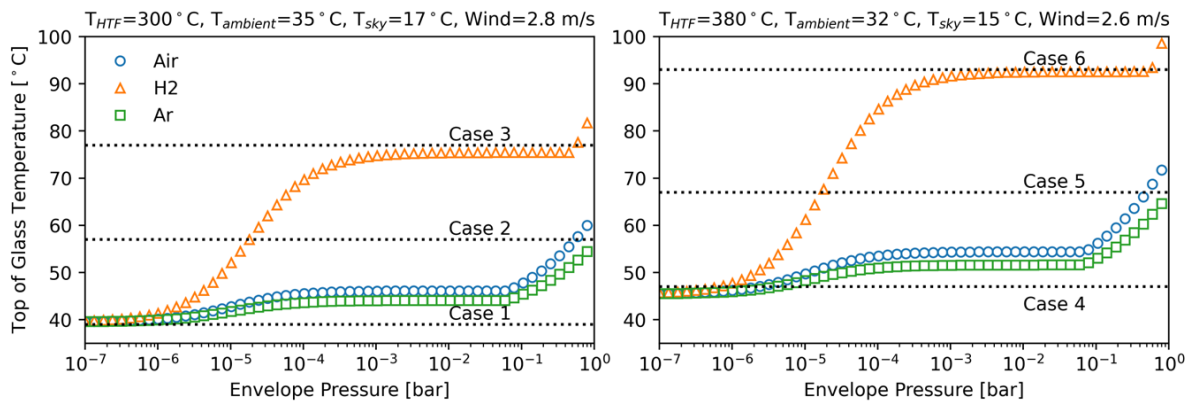


Figure 3. Glass temperature predicted by the Forristall model for representative cases at different HTF temperatures and annulus gas conditions, compared to measured survey data.

The horizontal dotted lines in Figure 3 correspond to the cases from Table 1. For the given conditions, it is evident that Case 3 and 6 are affected by H₂ infiltration, while Cases 1 and 4 appear to be well functioning HCEs. In comparison Cases 2 and 5 are difficult to interpret, both cases are in a temperature range that could be attributed to H₂ infiltration on the

order of $1e-5$ bar or air infiltration close to ambient pressure. Depending on the diagnosis different actions may be appropriate, e.g., argon injection is used to mitigate heat losses due to H_2 infiltration in some cases [1]. Figure 3 shows the benefits of argon injection, if the glass envelope is filled with atmospheric pressure argon the heat losses can be reduced significantly compared to hydrogen at $1e-3$ bar; however, these losses are still much higher than $P_{vac} < 1e-5$ bar.

Taking a closer look at Case 2, Figure 4 looks at parametric studies considering different glass envelope conditions. The most uncertain ambient parameters are the wind speed and sky temperature, which may have localized variations not captured in the available weather data. Case 2 can be modelled with H_2 infiltration in the glass envelope at a pressure of $2e-5$ bar, or with air at 0.6 bar based on the results plotted in Figure 4. At the conditions specified in Table 1 for Case 2, the sensitivity for both air and hydrogen cases are very similar. While the sensitivity to wind speed and sky temperature are of similar magnitudes, the trends are completely different. For a given set of conditions the sky temperature is proportional to the predicted glass temperature, in this case using an incorrect sky temperature close to ambient can increase the predicted glass temperature to levels where only H_2 infiltration may be expected. On the other hand, increasing the wind speed reduces the expected glass temperature, and the sensitivity is higher at lower wind speeds. When the average wind speed is relatively low, localized wind gusts have the potential to significantly lower the predicted glass temperature.

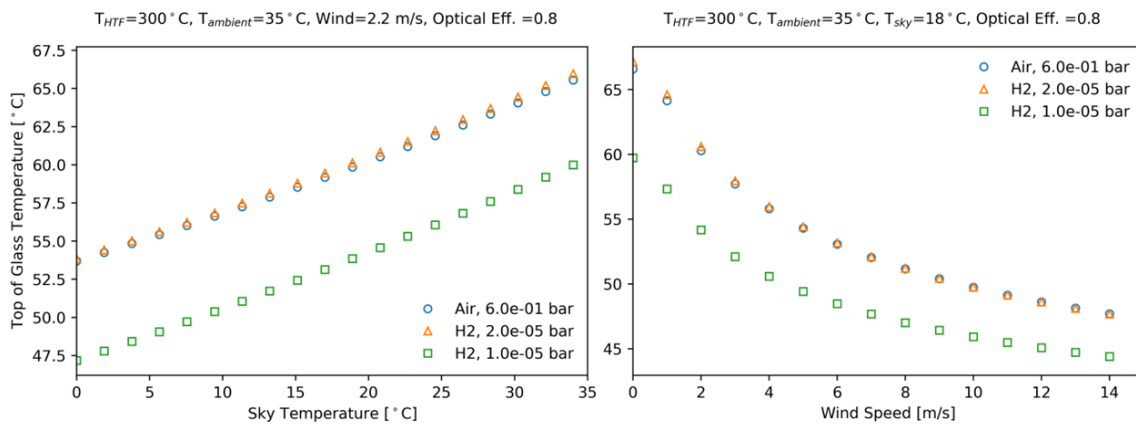


Figure 4. Model results considering the variation of uncertain ambient parameters.

Reviewing the results from Figure 3 and 4 it is not feasible to distinguish between a lost vacuum tube and H_2 infiltration at the ‘correct’ partial pressure. However, another aspect to consider is the getter capacity at different temperatures. Figure 4 shows how reducing the H_2 annulus pressure by half results in a significant change in the glass temperature regardless of ambient conditions. Thus, before the solar field warms up in the morning the measured glass temperature may correspond to a lower H_2 partial pressure compared to steady state operating conditions, allowing these HCEs to be identified with a comparative analysis.

4.3 Optical Properties

The optical properties of the absorber tube are another important parameter to consider when analyzing the measured temperature data. The selective coating on the absorber tube results in high absorption of solar energy, but low emittance for radiative heat losses. In addition to the absorber, the effective optical properties of the glass envelope itself may also vary due to soiling; dirt on the glass envelope can absorb energy that otherwise would have transmitted through. Figure 5 shows model results for different optical properties using the conditions from Case 2, but assuming full vacuum in the glass envelope. Although lowering the glass transmittance can have a measurable effect, the change in temperature is not sig-

nificant unless the absorptance of the glass also increases. If the absorptance increases a dirty HCE could result glass temperatures similar to Case 2 despite vacuum conditions. Likewise, as the absorber tube emittance approaches values for uncoated stainless steel the glass temperature increases significantly. When analyzing survey data it is important to consider the HCE optical properties when evaluating H₂ infiltration or lost vacuum.

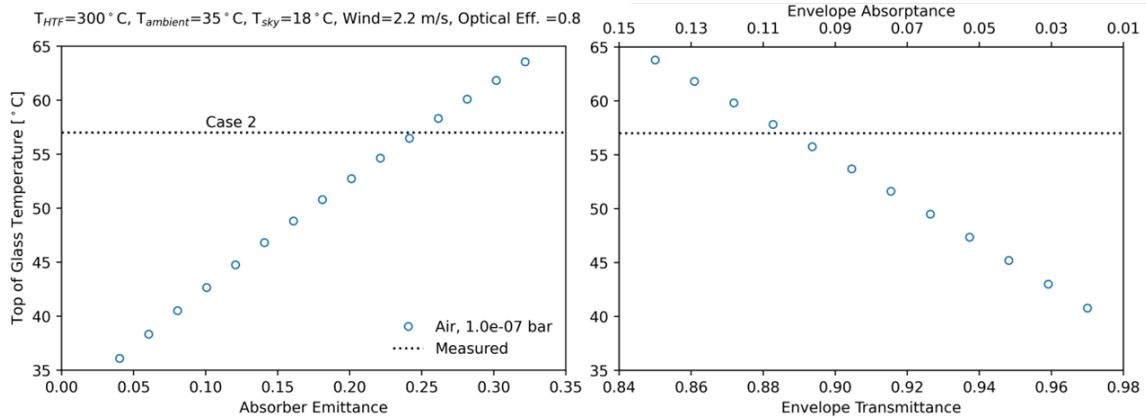


Figure 5. Model results for varying absorber tube emittance (left) and glass envelope transmittance (right), compared to the measured temperature of a potential lost vacuum HCE.

5. Conclusions

This work discusses the analysis of thermal survey data from operating parabolic trough plants using the 1D Forristall model to estimate HCE heat losses and glass envelope temperature. The reduced order model is less accurate at the higher heat loss conditions with an increase in the mean error of predictions from 0.7 to 4.9°C for glass temperatures > 20°C above ambient; although the increased error is of similar magnitude to the temperature measurement accuracy and not expected to impact predictions significantly, the model is being further developed to improve performance at these conditions. Results indicate the model is a useful and computationally efficient tool to determine the status of a given HCE; however, it can be difficult to distinguish between lost vacuum (from outside air infiltration), and H₂ infiltration (from decomposition of the HTF) between 1e-5 and 1e-4 bar. Parametric studies indicate similar behaviour of both these types of tubes for varying environmental conditions. The main methodology for identifying H₂ infiltration in these cases involves thermal surveying at different times of the day, taking advantage of the temperature dependence of the getter capacity.

Data availability statement

The data presented in this text is proprietary to Solar Dynamics LLC and the customer, which has also been kept confidential. Great care was taken to publish pictures and data relevant to the topics discussed that did not reveal any sensitive information.

Underlying and related material

The Forristall model was originally coded in EES [4], additionally a version of the model can be found in NREL's publicly available GitHub repository [10].

Author contributions

Luca Imponenti: writing – original draft, formal analysis, software

Keith Boyle: writing – review & editing, data curation, conceptualization

Ryan Shininger: writing – review & editing, investigation, project administration

Hank Price: writing – review & editing, supervision

Competing interests

The drone surveys and analysis described in this document are services sold by Solar Dynamics LLC and its partners.

Funding

This material is based upon work supported by the U.S. Department of Energy, Office of Science, Office of Small Business Innovative Research under Award Number DE-SC0021852.

Acknowledgement

The authors would like to thank the owners and operators of Nevada Solar One for access to facilities during development of the drone survey data collection and analysis.

References

1. M. Mehos et al., "Concentrating Solar Power Best Practices Study," Golden, CO, United States, 2020, <https://www.nrel.gov/docs/fy20osti/75763.pdf>. doi: <https://doi.org/10.2172/1665767>.
2. H. Price et al., "Field survey of parabolic trough receiver thermal performance," International Solar Energy Conference, 2006, vol. 3, pp. 1075–1082.
3. G. Glatzmaier, "Development of Hydrogen Mitigation for the Nevada Solar One Power Plant," Golden, CO, United States, 2020, <https://www.nrel.gov/docs/fy20osti/75127.pdf>.
4. R. Forristall, "Heat Transfer Analysis and Modeling of a Parabolic Trough Solar Receiver Implemented in Engineering Equation Solver," Golden, CO, United States, 2003. doi: <https://doi.org/10.2172/15004820>.
5. S. M. Akbarimoosavi and M. Yaghoubi, "3D thermal-structural analysis of an absorber tube of a parabolic trough collector and the effect of tube deflection on optical efficiency," Energy Procedia, vol. 49, pp. 2433–2443, 2014, doi: <https://doi.org/10.1016/j.egypro.2014.03.258>.
6. D. Lei, X. Fu, Y. Ren, F. Yao, and Z. Wang, "Temperature and thermal stress analysis of parabolic trough receivers," Renew. Energy, vol. 136, pp. 403–413, 2019, doi: <https://doi.org/10.1016/j.renene.2019.01.021>.
7. F. Burkholder and C. F. Kutscher, "Heat loss testing of Schott's 2008 PTR70 parabolic trough receiver," 2009, <http://www.nrel.gov/docs/fy09osti/45633.pdf>, doi: <https://doi.org/10.2172/1369635>.
8. F. Burkholder et al. "The test and prediction of argon-hydrogen and xenon-hydrogen heat conduction in parabolic trough receivers," Proceedings of SolarPACES Conference, Granada, Spain, 2011
9. J. A. Duffie & W. A. Beckman, "Selected Heat Transfer Topics," in Solar Engineering of Thermal Processes, 4th ed. Hoboken, NJ, United States: Wiley, 2013, ch. 3, sec. 1, pp 138-172

10. System Advisor Model Version 2021.12.02 (2021.12.02). SSC source code. National Renewable Energy Laboratory. Golden, CO. <https://github.com/NREL/ssc>